Experimental study of SO_2 emissions and desulfurization of oxy-coal combustion in a 30 kW_{th} pressurized fluidized bed combustor

Lei Pang[1], Yingjuan Shao[1,*], Wenqi Zhong[1], Hao Liu[2,**]

1. Key Laboratory of Energy Thermal Conversion and Control of Ministry of Education, School of Energy and Environment, Southeast University, Nanjing 210096, P.R. China
2. Department of Architecture and Built Environment, Faculty of Engineering, University of Nottingham, University Park, Nottingham NG7 2RD, UK

[*] Corresponding author
[**] Corresponding author
E-mail address: yjshao@seu.edu.cn (Y. Shao), Liu.Hao@nottingham.ac.uk (H. Liu)

Abstract

Pressurized oxy-fuel combustion (POFC) has attracted wide attention due to its potentials of high efficiency and low cost in CO_2 capture. Compared with numerical simulation and system analysis, there are few experimental studies about POFC. In order to investigate the SO_2 emissions and desulfurization behaviors of limestone under continuous fuel-feeding POFC conditions, a series of oxy-coal combustion experiments were conducted with a 30 kW_{th} pressurized fluidized bed combustor. The results showed that the SO_2 emission was almost independent of combustion pressure and excess oxygen coefficient, while it was higher in air than in O_2/CO_2 atmosphere because less sulfur was retained by the coal ash. Although the higher CO_2 partial pressure caused by an increase in combustion pressure from 0.1 MPa to 0.4 MPa had negative effects on the calcination of limestone and inhibited the indirect desulfurization, the higher combustion pressure was beneficial to improve the direct desulfurization efficiency. An increase in combustion temperature from 850 ^oC to 950 ^oC significantly improved the desulfurization efficiency of limestone with both atmospheric and pressurized oxy-coal combustion. SEM images were obtained and used to show the surface morphology of limestone products under different combustion conditions, which was helpful to the understanding of the desulfurization behaviors of limestone.

Keywords: SO_2 emissions; Desulfurization; Oxy-coal combustion; Pressurized fluidized-bed.

1. Introduction

Oxy-fuel combustion has been widely accepted as a highly-effective CO_2 capture and storage (CCS) technology [1-3], and a combination of this technology with fluidized beds, i.e., oxy-fuel combustion in fluidized beds, has attracted a lot of attention from researchers during last decade due to its inherent advantages in fuel flexibility, in-furnace desulfurization and low NO_x emissions [2, 4-5]. Although oxy-fuel combustion-based CCS can still lead to a reduction of about 10% in the net plant efficiency [6], pressurized oxy-fuel combustion (POFC) has been proposed as an option to improve the efficiency [7]. Many performance analyses of POFC have concluded that an increase in combustion pressure can decrease the reduction of the net plant efficiency resulted from oxy-fuel combustion-based CCS as the higher combustion pressure is helpful to recover more thermal energy from the flue gas and reduce the energy cost of CO_2 compression work [8-10]. The limited experimental investigations on POFC conducted so far have showed that increasing the combustion pressure can not only improve the combustion rate and combustion efficiency [11-12] but also reduce NO_x emissions [13].

In-furnace desulfurization by use of a sulfur capture sorbent such as limestone is one of the most important features with fluidized bed combustion. Therefore, the studies of oxy-fuel combustion in fluidized beds must address in-furnace desulfurization and emissions of SO_2 which is a main precursor to acid rain. High concentrations of SO_2 in the flue gas can cause not only the corrosion of devices/pipes but also negative impacts on CO_2 compression and purification. SO_2 emission behaviors with atmospheric oxy-fuel combustion have been widely studied [14-20]. For example, the SO_2 concentration

in the flue gas under atmospheric O_2/CO_2 atmosphere was found to be higher than that under air due to the recycled flue gas [14-16]. Several studies [17-19] found that the SO_2 emission under O_2/CO_2 atmosphere was about 15-30% less than that under air, with the decrease of SO_2 emission being attributed to more SO_2 being absorbed by the condensate water or retained by the ash under the O_2/CO_2 atmosphere. On the other hand, Liu et al. [20] showed that the SO_2 emission was almost independent of the atmosphere, air or O_2/CO_2. Possible reasons for these conflicting results may include the differences in the oxy-fuel combustion systems and the properties of fuel ash between these previous investigations. Furthermore, previous experimental results have shown that the excess air/oxygen, combustion temperature and O_2 concentration in the oxidizer have insignificant effects on SO_2 emissions under atmospheric O_2/CO_2 atmosphere once the steady combustion condition is achieved [21-23].

Fluidized bed combustion is well-known for its economical desulfurization by introducing calcium based sorbents (e.g. limestone) into the furnace [24-25]. In a traditional FB combustor of air combustion, the calcination of limestone occurs prior to the desulfurization reaction (indirect desulfurization: Reactions 1-2). However, the higher CO_2 partial pressure in oxy-fuel combustion may hinder the proceeding of calcination, and sulfurization may occur directly between $CaCO_3$ and SO_2 (Reaction 3) [24].

$$CaCO_3 \rightarrow CaO+CO_2 \quad (1)$$

$$CaO+SO_2+\frac{1}{2}O_2 \rightarrow CaSO_4 \quad (2)$$

$$CaO_3 + SO_2 + \frac{1}{2}O_2 \rightarrow CaSO_4 + CO_2 \quad (3)$$

The two different sulfurization routes, indirect and direct, are mainly determined by the CO_2 partial pressure and the combustion temperature [24-25]. It has been proved that the higher CO_2 concentration in the flue gas of oxy-fuel combustion could lead to the transition from indirect sulfurization to direct sulfurization, reducing the reaction rate as well as desulfurization efficiency dramatically [26-28]. According to the equilibrium theory [24-25], the calcination temperature of limestone increases with CO_2 partial pressure. Therefore, one effective method to increase the desulfurization efficiency of oxy-fuel combustion is to increase the combustion temperature. Previous investigations [29-30] had showed that when the temperature was increased from 850 ^oC to about 920 ^oC, the indirect desulfurization occurred, and the overall desulfurization efficiency increased significantly. In addition to the experiments conducted in FB combustors mentioned above [14, 17, 21, 26-29], Kim et al. [25], Jeong et al. [24] and Francisco et al. [31] had also investigated the desulfurization mechanisms and behaviors of limestone by using thermo-gravimetric analyzers. It was found that the direct desulfurization reaction rate increased with the temperature while that of indirect desulfurization was hardly affected by the temperature. Besides, the product layer and pore structure formed on the surface of sorbents affect the desulfurization reaction significantly. The particle size of the sorbents and SO_2 concentration also play important roles in the desulfurization process under oxy-fuel combustion conditions, and generally the desulfurization efficiency decreases with sorbent particle size but increases with an increase in SO_2 concentration [32]. In theory, an increase in

combustion pressure will increase the CO_2 partial pressure, which may cause negative effects on the desulfurization. However, there are few experimental investigations about the SO_2 emission and desulfurization under POFC conditions to elucidate the effect of combustion pressure on desulfurization. This knowledge gap can significantly hinder the development of POFC technology as the knowledge is indispensable for the conceptual design of SO_2 control strategies for POFC systems.

This study investigates the SO_2 emission behaviors of both air and oxy-coal combustion in a 30 kW_{th} fluidized bed combustor under different POFC conditions. The effects of combustion atmosphere, pressure and temperature on the desulfurization of limestone were investigated thoroughly. Scanning electron microscopy (SEM) and nitrogen adsorption analysis were used to characterize the surface structures of limestone under different POFC conditions.

2. Experimental

2.1 Experimental setup

The SO_2 emission and desulfurization experiments of this study were carried out with a 30 kW_{th} pressurized fluidized bed combustion system shown in Fig. 1(a), which had been described elsewhere [33]. As it was too difficult to separate the limestone products with the coal ash and bed materials after the combustion experiments in the fluidized bed system, a pressurized tube furnace system [34] (Fig. 1(b)) was used to investigate the surface structure of limestone under the same pressures and atmospheres as those in the fluidized bed combustor.

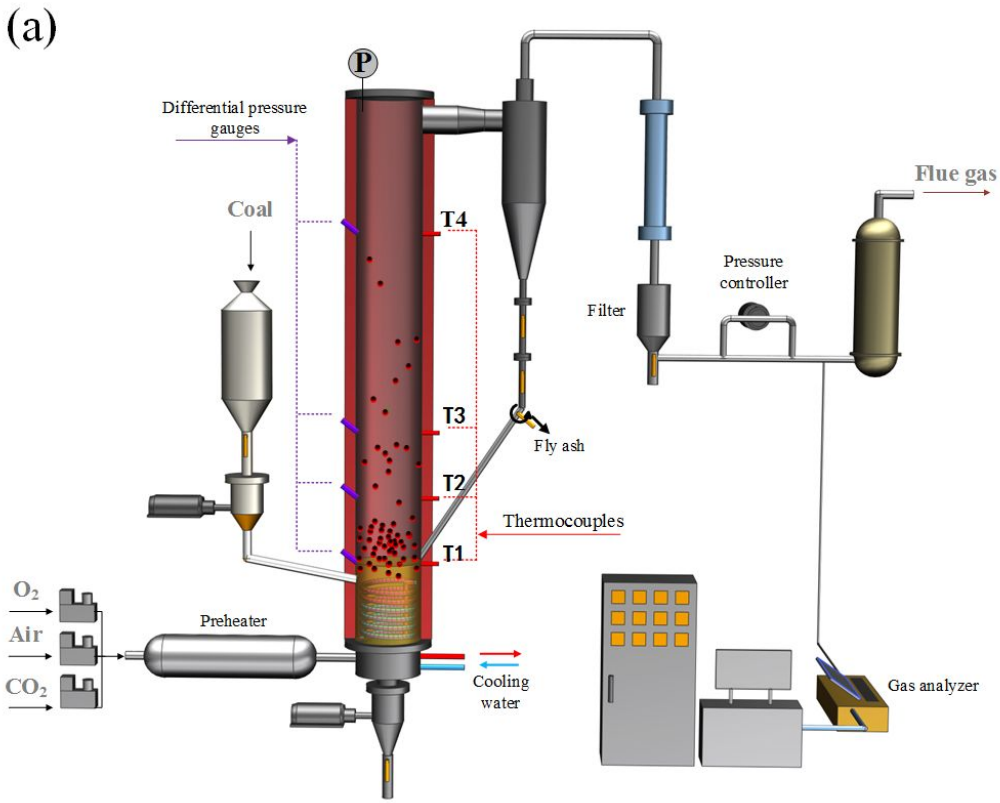

Figure 1. Scheme of (a) POFC system (b) pressurized tube furnace system

2.2 Fuel and material

One typical anthracite from Shanxi province, China, was used in all of the tests. Table 1 gives the analysis of the coal sample. Silica sand with the particle size ranging from 0.4 mm to 1.6 mm was used as the bed material. The limestone used in this study mainly consists of $CaCO_3$ and its composition is presented in Table 2. Fig. 2 shows the

size distributions of the coal, silica sand and limestone particles.

Table 1. Ultimate analysis and proximate analysis of the anthracite coal

	Anthracite
Proximate Analysis (wt%, as received)	
Moisture	2.51
Ash	14.09
Volatile matter	10.44
Fixed carbon (by difference)	72.96
Ultimate Analysis (wt%, as received)	
Carbon	76.83
Hydrogen	2.30
Nitrogen	0.94
Sulfur	1.30
Oxygen (by difference)	2.03

Table 2. The main composition of limestone sample

Composition	**$CaCO_3$**	**SiO_2**	**Al_2O_3**	**Fe_2O_3**	**MgO**
Content (wt %)	**92.31**	**3.20**	**1.83**	**1.20**	**0.79**

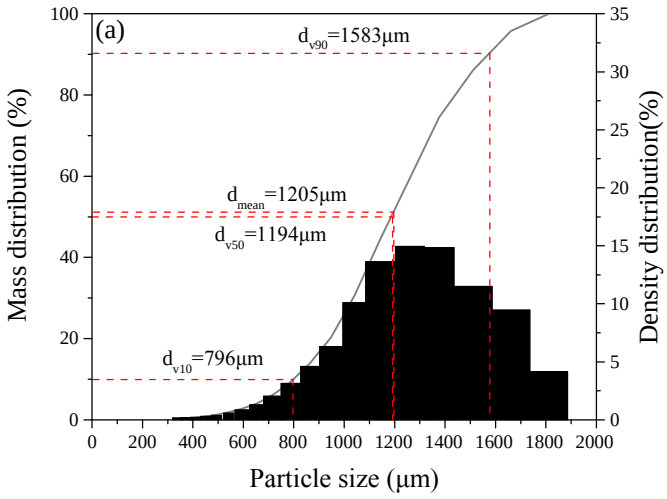

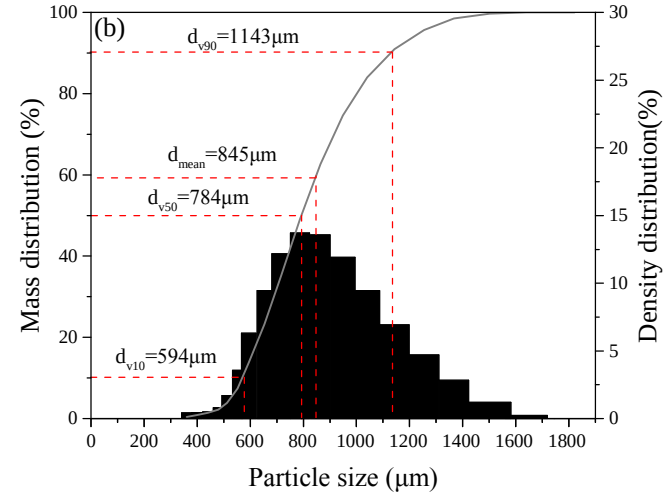

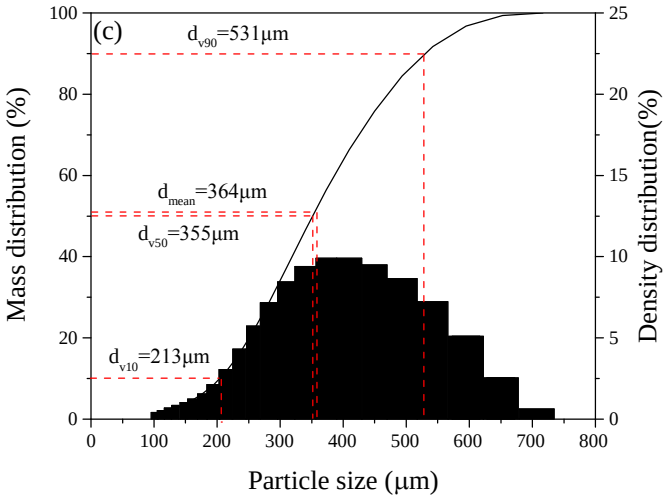

Figure 2. Particle size distribution of (a) coal particle (b) silica sand (c) limestone

2.3 Procedure

2.3.1 SO_2 emission and desulfurization

Table 3 (a) shows the operating parameters of all tests. The total weight of the bed materials (silica sand) was fixed at 1.5 kg for all tests which included atmospheric air, atmospheric oxy-fuel, pressurized air and pressurized oxy-fuel combustion tests. In order to keep the superficial gas velocity and excess oxygen at the same level between different tests, the coal feeding rate and oxidant flow rate were increased in proportion

146 to the combustion pressure and the bed temperature was controlled by the water cooling
147 system. Tests without limestone (Ca/S = 0) were used to study the SO_2 emission
148 behaviors while tests with the Ca/S molar ratio of 2.5 were carried out to investigate
149 the desulfurization efficiency of limestone under different conditions. The SO_2
150 concentration in the flue gas was measured by using a flue gas analyzer (MADUR GA-
151 21 plus) with the SO_2 measuring module (measuring range: 0 - 5000 ppm and the
152 precision is 1 ppm), and all the experimental results were ensured by repeated runs.

153 **2.3.2 Surface structure of limestone**

154 A crucible loaded with 1 g limestone particles was first placed in the unreactive
155 zone of the pressurized tube furnace, and then the reactor was sealed under room
156 temperature. Before the furnace was heated, the reactant gas was introduced, and the
157 pressure was controlled to a desired level. The crucible containing limestone particles
158 was pushed into the reaction zone by the push rod after the temperature reached the
159 target value. After 2 hours, the heater was turned off, and the inlet gas was switched to
160 N_2 while the pressure was maintained constant. When the temperature dropped to 300
161 ^{o}C, the crucible was taken out, and the products in the crucible were collected.
162 Afterwards, the products were characterized by a scanning electron microscopy (S-
163 3400N II) and a nitrogen adsorption analyzer (ASAP 2020M). Table 3 (b) summarizes
164 the operating parameters of the pressurized tube furnace tests.

Table 3 (a). Operating parameters and dry flue gas compositions of POFC experiments

Pressure (MPa)	O_2 in (vol %)	CO_2 in (vol %)	Fuel input (kg/h)	Total gas flow (NM^3/h) *	Superficial gas velocity (m/s)* *	Ca/S	T1 (°C)	O_2 out (vol %)	CO_2 out (vol %)	SO_2 (ppm)
0.1	**Air**	**Air**	**0.65**	**4.5-6.0**	**1.05-1.42**	**0**	**880-900**	**2.0-6.0**	**14-19**	**970-1250**
0.1	**25**	**75**	**0.65**	**4.8-5.6**	**1.14-1.35**	**0**	**900-920**	**3.4-6.2**	**90-93**	**820-966**
0.1	**30**	**70**	**0.60**	**3.3-4.0**	**0.78-0.96**	**0**	**900-910**	**2.3-6.5**	**90-94**	**1050-1230**
0.1	**Air**	**Air**	**0.50-0.65**	**4.5-6.0**	**0.99-1.42**	**2.5**	**815-900**	**3.0-4.2**	**17-18**	**130-200**
0.1	**30**	**70**	**0.50-0.70**	**3.0-4.3**	**0.68-1.06**	**2.5**	**840-950**	**2.8-3.6**	**92-94**	**300-1000**
0.4	**Air**	**Air**	**2.70**	**21.0-26.0**	**1.23-1.56**	**0**	**880-910**	**2.1-6.4**	**14-19**	**920-1150**
0.4	**30**	**70**	**2.50**	**14.0-16.8**	**0.82-1.00**	**0**	**880-900**	**1.9-6.8**	**89-94**	**990-1200**
0.4	**Air**	**Air**	**2.1-2.6**	**21.5-26.0**	**1.18-1.54**	**2.5**	**815-900**	**2.7-4.0**	**17-18**	**320-650**
0.4	**30**	**70**	**2.50-2.80**	**16.1-18.4**	**0.91-1.14**	**2.5**	**840-950**	**2.5-6.8**	**89-93**	**300-780**

* NM^3/h – cubic meter per hour under standard conditions (0 °C and 1 atm)

**Superficial gas velocities were calculated on the basis of the measured bed zone temperature T1

168 **Table 3 (b). Operating parameters of pressurized tube furnace experiments**

Pressure (MPa)	O_2 in (vol %)	CO_2 in (vol %)	SO_2 (ppm)	Temperature (°C)
0.1	**Air**	**Air**	**0**	**850**
0.1	**30**	**70**	**0**	**850, 900, 950**
0.1	**30**	**70**	**800-1000**	**850, 950**
0.4	**Air**	**Air**	**0**	**850, 900**
0.4	**30**	**70**	**0**	**850, 900, 950**
0.4	**30**	**70**	**800-1000**	**850, 950**

169

170 **2.4 Calculation method**

171 The percentages of Coal-S converted to SO_2 and retained by the coal ash can be
172 calculated using Equations 4-6:

$$C_{S\rightarrow SO_2} = \frac{[SO_2]_{fg}}{[S]_{coal}} \times 100\% \quad (4)$$

$$C_{S\rightarrow ash\text{-}organic\text{-}S} = \frac{[organic\text{-}S]_{ash}}{[S]_{coal}} \times 100\% \quad (5)$$

$$C_{S\rightarrow ash\text{-}sulfate\text{-}S} = \frac{[sulfate\text{-}S]_{ash} - [sulfate\text{-}S]_{coal}}{[S]_{coal}} \times 100\% \quad (6)$$

173 Where $[SO_2]_{fg}$, $[sulfate\text{-}S]_{ash}$, $[organic\text{-}S]_{ash}$, $[sulfate\text{-}S]_{coal}$ and $[S]_{coal}$ represent the
174 molar SO_2 in the flue gas, the molar sulfur as sulfate in the coal ash, the molar sulfur as
175 organic sulfur in the coal ash, the molar sulfur as sulfate in the feeding coal and the
176 molar sulfur as organic sulfur in the feeding coal (per unit time), respectively. [organic-
177 S] and [sulfate-S] were obtained by elemental analysis (Table 1, Table 4 (a)) and X-ray
178 fluorescence (XRF) analysis (Table 4 (b), Table 5), respectively.

179 The desulfurization efficiency of limestone (η) is commonly calculated by the
180 Equation (7) [26]:

$$\eta = (1 - \frac{[SO_2]_{fg}}{[S]_{coal}}) \times 100\% \quad (7)$$

It is worth mentioning that not all the sulfur in coal can be converted to SO_2, and the minimum value of η is not zero even though no limestone is introduced. As shown later in Section 3.1, the coal ash has some sulfur retention ability, and the desulfurization efficiency without limestone addition is the self-desulfurization efficiency of the coal ash. In order to separate the desulfurization of the coal ash from that of limestone, the desulfurization efficiency of limestone was calculated by Equation (8):

$$\eta = (1 - \frac{[SO_2]_{fg,\ with\ limestone}}{[SO_2]_{fg,\ no\ limestone}}) \times 100\% \quad (8)$$

Where $[SO_2]_{fg,with\ limestone}$ and $[SO_2]_{fg,no\ limestone}$ represent the molar SO_2 in the flue gas with and without limestone injection (per unit time), respectively.

Table 4 (a). Elementary analysis of ashes (no addition of limestone)

Ash type	Pressure (MPa)	Atmosphere	C (%)	N (%)	H (%)	S (%)
Cyclone ash	0.1	Air	45.1	0.27	0.44	0.59
	0.1	Oxy-30	39.9	0.22	0.41	0.66
	0.4	Air	35.5	0.18	0.23	0.60
	0.4	Oxy-30	32.3	0.14	0.20	0.58
Bottom ash	0.1	Air	0.24	0.06	0.53	0.50
	0.1	Oxy-30	0.80	0.06	0.50	0.58
	0.4	Air	0.43	0.07	0.28	0.42
	0.4	Oxy-30	0.71	0.05	0.26	0.53
Residual ash (filter ash)	0.1	Air	50.1	0.27	0.41	0.61
	0.1	Oxy-30	43.9	0.21	0.38	0.69
	0.4	Air	39.5	0.16	0.20	0.58
	0.4	Oxy-30	37.3	0.13	0.18	0.60

Table 4 (b). Primary chemical composition of cyclone ashes (no addition of limestone)

Pressure (MPa)	Atmosphere	Mass loss (%)	SiO_2 (%)	Al_2O_3 (%)	Fe_2O_3 (%)	CaO (%)	SO_3 (%)
0.1	Air	45.12	24.07	22.03	3.65	1.89	2.49
0.1	Oxy-30	39.73	26.14	23.19	3.78	2.29	4.20
0.4	Air	35.50	28.75	26.26	3.91	2.82	2.39
0.4	Oxy-30	32.37	29.08	25.53	4.24	2.92	4.83

Table 5. The main composition of the coal sample

Composition	Mass loss	SiO_2	Al_2O_3	Fe_2O_3	CaO	SO_3
Content (wt %)	84.79	6.46	5.68	0.91	0.57	0.32

3. Results and discussion

3.1 SO_2 emissions

Fig. 3 (a) and (b) show the real-time data of temperatures and gas concentrations for some typical experiments. It should be noticed that the SO_2 concentration in the flue gas cannot be used to compare the SO_2 emission between different combustion atmospheres because it is also affected by the gas flow rate. For example, Fig. 3(a) shows that the SO_2 concentrations of coal combustion in air and 25% O_2/75% CO_2 (oxy-25) were at almost the same value, i.e., about 1000 ppm, but the total gas flow rate of oxy-25 was lower than that of air in order to keep the same oxygen flow rate, and hence the SO_2 emission actually reduced when the oxidant was switched from air to oxy-25.

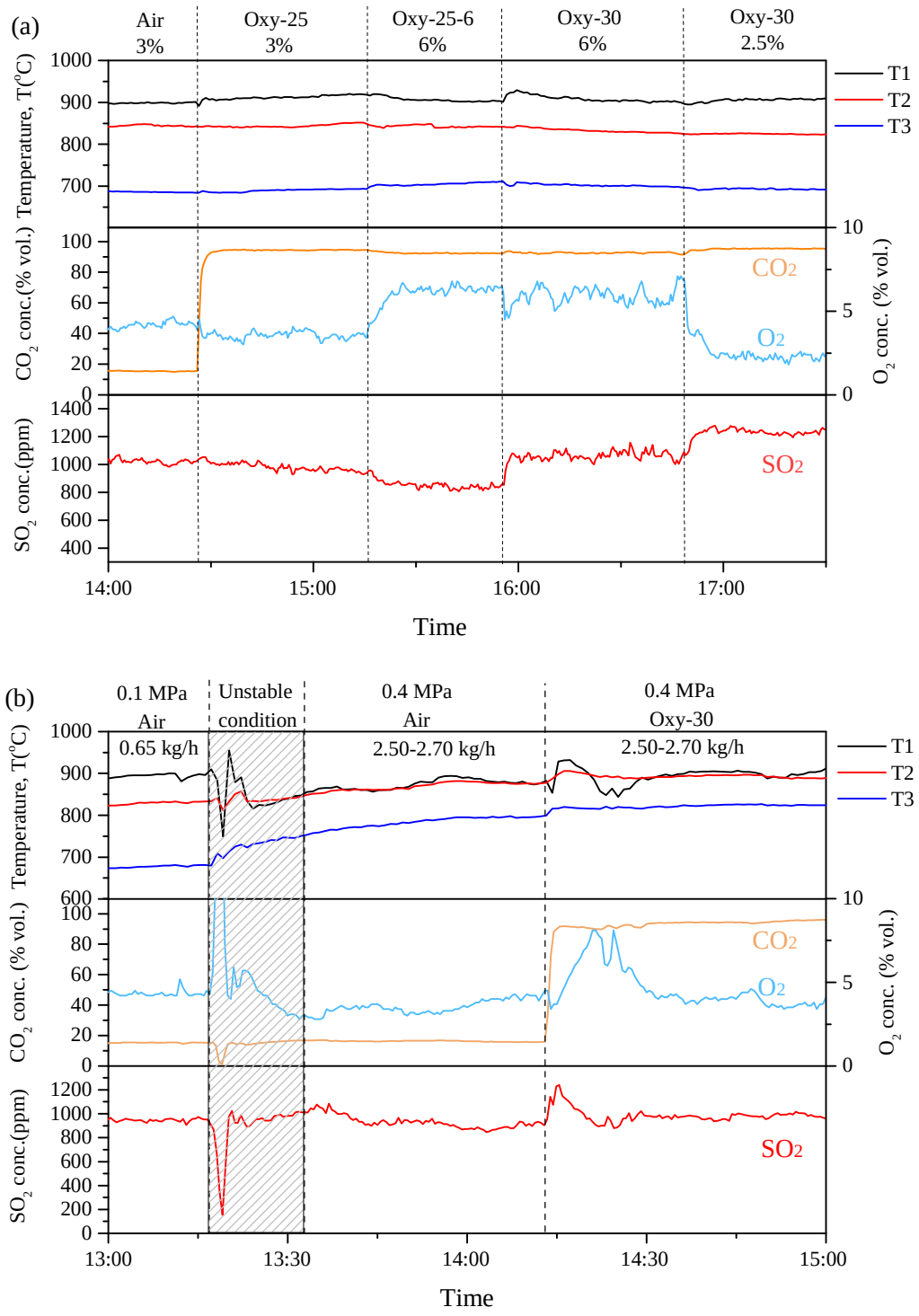

Figure 3. Real-time data of temperatures and flue gas without limestone (a) 0.1 MPa with the coal feeding rate of 0.60-0.65 kg/h (b) 0.4 MPa with the coal feeding rate of 2.50-2.70 kg/h

Fig. 4 compares the SO_2 emissions with the normalized emission per energy unit under different combustion atmospheres and pressures. The SO_2 emission decreased

218 from 837 mg/MJ to 716 mg/MJ (representing a reduction of 14.46%) when the
219 combustion atmosphere was switched from air to 30% O_2/70 % CO_2 (oxy-30) under
220 atmospheric pressure, which was in agreement with most previous studies. Although
221 the uncertainty associated with SO_2 measurement and fluctuations (up to 6%) could not
222 be ignored, the decrease of SO_2 emissions resulted from the switch of air combustion
223 to oxy-coal combustion was considered to be significant and much bigger than the
224 uncertainty. Zou et al. [17] found that the SO_2 emission under 27.3 % O_2/72.7 % CO_2
225 condition was 15.7% less than that in air, and Croiset et al. [18] also showed the
226 conversion ratio of coal-S to SO_2 dropped from 91% to 75% when the combustion
227 atmosphere was switched from air to O_2/CO_2 mixtures. As less coal-S was emitted as
228 SO_2 in oxy-fuel combustion, some researchers analyzed the ash sample and found a
229 higher fraction of organic-S or sulfate in ash [19, 36]. Besides, Croiset et al. [18]
230 indicated that the condensed water of oxy-fuel combustion had a higher concentration
231 of sulfates. Fig. 5 (a) shows the mass fractions of the bottom ash, cyclone ash and
232 residual ash under different combustion conditions. Because the size of coal particles
233 used in this study was small (0.4-1.8 mm), only a small portion of the total coal ash was
234 left in the combustor. The mass fraction of the bottom ash was less than 3% and most
235 of the coal ash was collected by the cyclone. The cyclone ash and bottom ash accounted
236 for about 80% of the total coal ash. The remaining part of the total coal ash is defined
237 in this study as the residual ash which includes the ash in the filter, in the deposits of
238 the flue-gas cooler and tubes as well as the part of the fly ash which has not been
239 collected by the cyclone or filter, i.e. which has escaped with the flue gas. The detailed
240 ash collection process was described in our previous study [33]. Fig. 5 (b) shows the
241 percentage of the coal-S retained in the ash as the organic sulfur which was calculated
242 on the basis of mass fraction and elemental analysis of different types of ashes (Table 4

(a)). It is worth mentioning that the mass fraction of organic sulfur element in the residual ash was assumed to be the same as that of the filter ash which represented 50-70% of the residual ash. Although the overall percentage of coal-S retained as organic sulfur in ashes was slightly lower under 0.4 MPa than that under 0.1 MPa, there was no obvious difference between air combustion and oxy-30 combustion with the same pressure. As the elemental analysis is not able to determine the sulfates in ashes, X-ray fluorescence (XRF) analysis was used to identify the ash composition including the sulfate, and the results are shown in Table 4 (b). The percentages of SO_3 in ashes of oxy-30 combustion were much higher than those of air combustion under the same combustion pressure, which explains the lower SO_2 emissions in oxy-30. Fig. 6 shows the sulfur mass balance which included SO_2 in the flue gas and the organic S and sulfates in all of the ashes. It is clear that more sulfur was converted to sulfates in ashes under oxy-30 combustion, which lead to a lower SO_2 emission. Some researchers [18] attributed the higher S content in coal ash with oxy-coal combustion to the higher SO_2 concentration in flue gas, as the higher SO_2 concentration in the flue gas is beneficial to the conversion of SO_2 to sulfates. However, the SO_2 concentration in the flue gas under oxy-30 combustion condition was only 10-20% higher than that of air combustion in this study due to the lack of recycled flue gas. The longer gas-ash contact time under the oxy-combustion conditions should have also improved the formation of sulfates in the ashes [19]. It has been noticed that the sulfur mass balance in Fig. 6 was still not completely closed in this study. Possible sources of unaccounted sulfur mainly include the sulfur retained in water and the sulfur converted to SO_3 (gas). As not all of the residual ash was collected, the mass fraction of sulfur element in all residual ash was assumed to be the same as that of the filter ash despite of the fact that the filter ash only represented 50-70% of all residual ash. According to Fleig et al. [19], the ash samples

collected from the reactor wall and cooling tubes had a much higher S content than that of the filter ash. Therefore, the actual amounts of sulfur retained in the residual ash could be higher than the calculated values shown in Figs. 5-6.

Fig. 4 also compares the SO_2 emissions under different combustion pressures with the same atmosphere. In order to eliminate other parameters' effects, the bed temperature was kept at about 900 ^oC while the oxygen concentration in the flue gas was kept at about 3-4 vol%. The SO_2 emission was almost independent of the combustion pressure as it showed negligible changes when the pressure was increased from 0.1 MPa to 0.4 MPa under the same combustion atmosphere. A recent study from Duan et al. [37] showed that the SO_2 emission decreased dramatically with an increase in combustion pressure, and the author attributed the reduction of SO_2 emission to the enhanced self-desulfurization of ash under high pressures. However, a trend similar to that of Duan et al. [37] was not observed in this study. Self-desulfurization is mainly determined by the quantities of alkali and alkaline earth metals (Na, K, Mg, Ca) in the fuel ash but the coal used in this study is different from the coals used by Duan et al. [37] both in terms of rank and ash content, and this should have contributed to the difference in the effect of pressure on the SO_2 emission between this study and Duan et al. [37]. Since the pressure had an insignificant impact on SO_2 emissions, the conversion of SO_2 to SO_3 in this study should be very small even though the previous simulation study [38] had showed that up to about 20% of SO_2 could be converted to SO_3 under the pressure of 1.5 MPa at 900 ^oC. As already pointed out, the SO_2 emissions of air combustion were always higher than those of oxy-fuel combustion under the same combustion pressure, whether at atmospheric or pressurized condition.

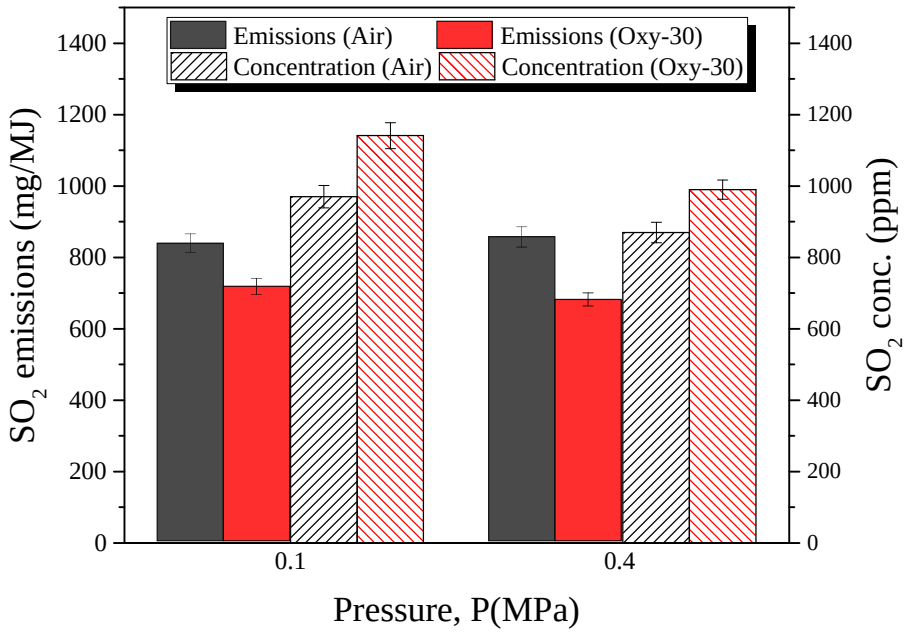

291
292 Figure 4. SO_2 emissions (T1: 880-900 ^oC, O_2: 3-4 vol%)
293

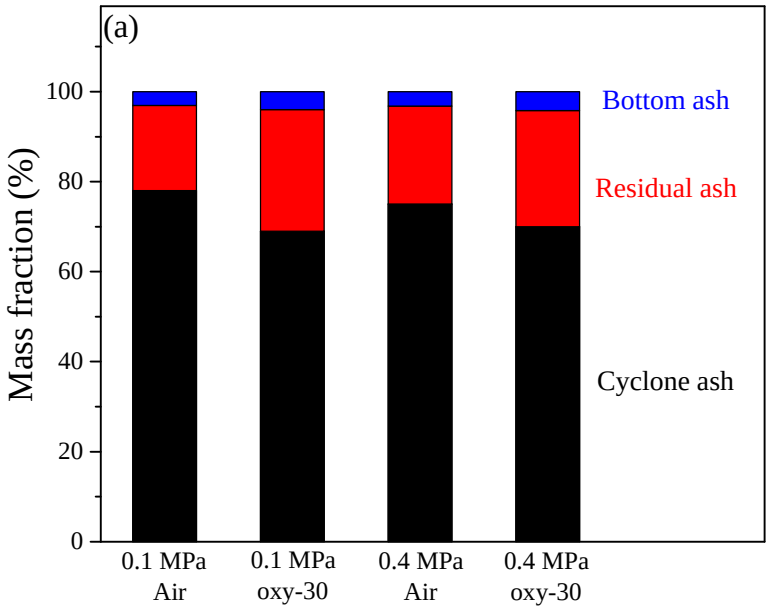

294

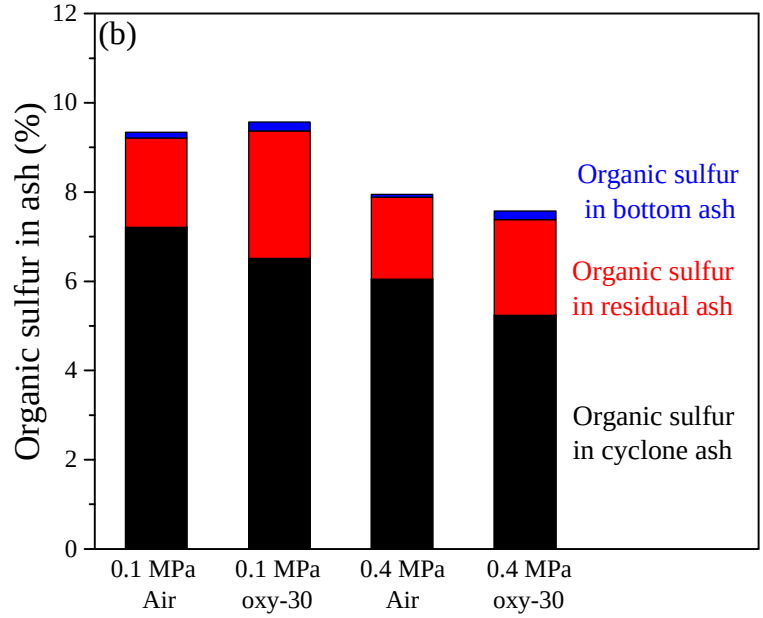

Figure 5. (a) Mass fraction of different types of ash (b) Organic sulfur in ash (T1: 880-900 ºC, O_2: 3-4 vol%)

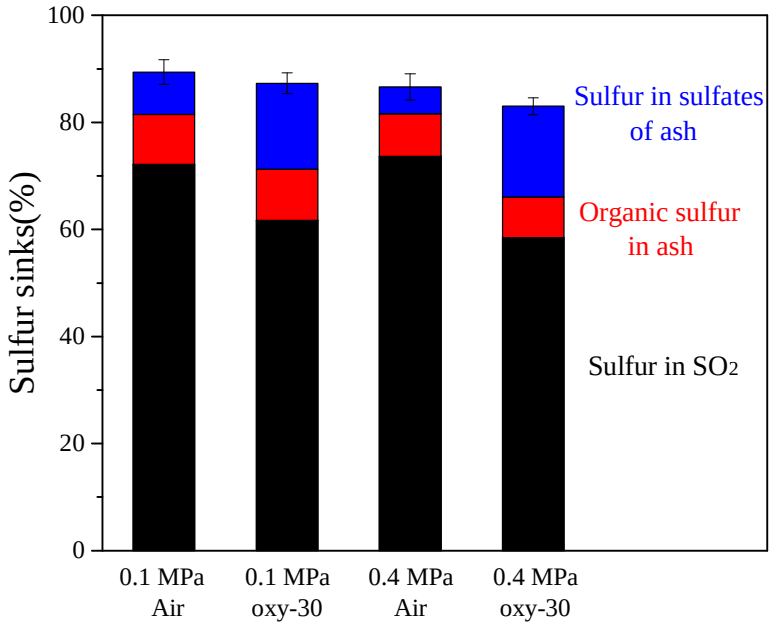

Figure 6. Sulfur mass balance (T1: 880-900 ºC, O_2: 3-4 vol%)

Several previous studies proved that the excess air/oxygen played an important role in CO and NO_x emissions under both atmospheric air and oxy-fuel combustion conditions [35, 39], whereas the experimental results from Tan [21] showed that the SO_2 emission remained stable when the excess oxygen ratio was increased from 1.05 to 1.20. Fig. 7 shows the effect of excess oxygen level in the flue gas on SO_2 emissions. Although the uncertainty associated with SO_2 emissions was about 50 mg/MJ, which was largely caused by the fluctuations of coal feeding rate, air or O_2/CO_2 mixture flow rate and combustion in the fluidized bed combustor, there was no obvious change in SO_2 emission being observed under both pressures of 0.1 MPa and 0.4 MPa when the oxygen concentration in the flue gas was increased from 2 vol% to 7 vol%. This indicates that the excess oxygen level of the combustion had little effect on the SO_2 emissions under the conditions of this study. It is worth mentioning that this conclusion was drawn on the basis of a good coal burnout being maintained under all excess oxygen levels (the carbon mass loss of the coal [33] can be calculated by using the data shown in Table 1 and Table 4, and it was about 85%-92% in this study, which indicates a good coal burnout). If the coal was far away from complete burnout in the combustor, a large quantity of combustibles would be contained in the bottom ash and fly ash and an increase in excess oxygen would promote the combustion efficiency, hence increase the SO_2 emissions significantly.

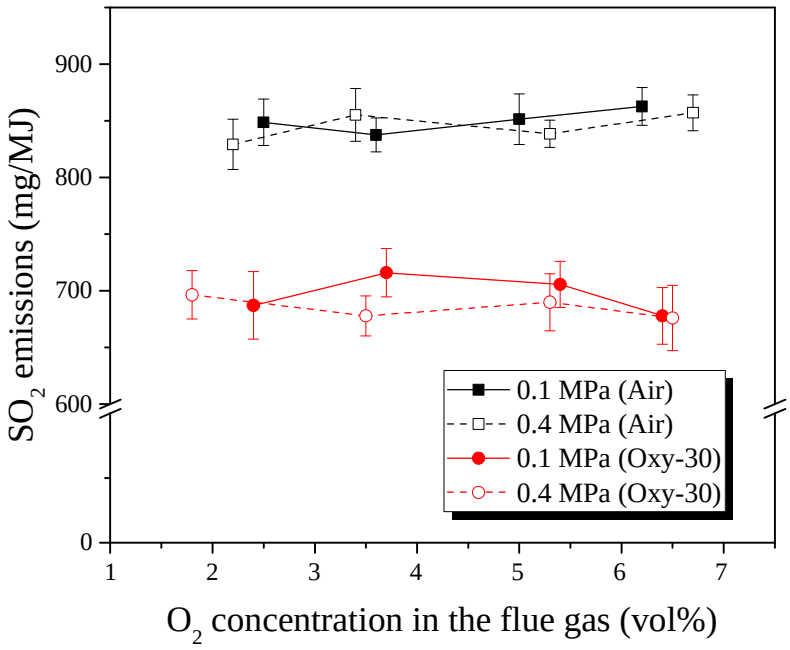

Figure 7. SO_2 emissions with different excess oxygen levels (T1:880 ºC - 900 ºC)

3.2 Desulfurization of limestone

One of the advantages of fluidized bed combustion is the in-furnace desulfurization by introducing limestone into the combustor directly, and its efficiency can reach up to 90% [2]. Fig. 8 shows the equilibrium curve of $CaCO_3$ calcination which is highly dependent on the CO_2 partial pressure and temperature [24-25]. In traditional atmospheric air FB combustion, the reaction condition leads to the indirect desulfurization, i.e., a step of calcination of limestone (Reaction 1) occurs before SO_2 is captured by CaO (Reaction 2), instead of $CaCO_3$ (Reaction 3). Fig. 9 (a) shows the real-time data of temperatures and gas concentrations for one test with limestone injection (Ca/S=2.5). It can be seen that the SO_2 concentration of air combustion reduced to about 160 ppm whereas it was about 1000 ppm without limestone (Fig. 3 (a)), and the desulfurization efficiency was over 80%. Although the bed temperature was kept at the same level (880 ºC), the SO_2 concentration increased constantly to 750 ppm after the oxidant was switched from air to oxy-30, and the desulfurization

efficiency decreased dramatically to 55%. The lower desulfurization efficiency of limestone in oxy-fuel combustion has also been observed by many other researchers [26-28]. Jia et al. [28] found that the sulfur capture efficiency dropped from 86% (air) to 65% (oxy-34), and Lupianez et al. [27] reported a decline of 18% from air to oxy-25. Because the CO_2 concentration in the flue gas was about 85-90 vol% in oxy-fuel combustion conditions, the CO_2 partial pressure was 80-90 kPa, and the calcination of limestone cannot occur unless the temperature reaches about 900 ^{o}C. As many experiments [45] have proved that the surface of CaO particle is much more porous than that of $CaCO_3$ due to the release of CO_2 during the calcination process, SO_2 can enter the inner part of the CaO particle easily, which increases the sulfur capture capacity. Therefore, the transition from indirect to direct desulfurization led to the lower sulfur capture efficiency in oxy-fuel combustion. As shown in Fig. 9 (a), the SO_2 concentration decreased from 750 ppm to 300 ppm after the bed temperature was increased from 880 ^{o}C to about 940 ^{o}C. The higher temperature allowed the limestone to decompose into CaO and CO_2 (Reaction 1) under the oxy-fuel combustion condition, and hence increased the sulfur capture efficiency.

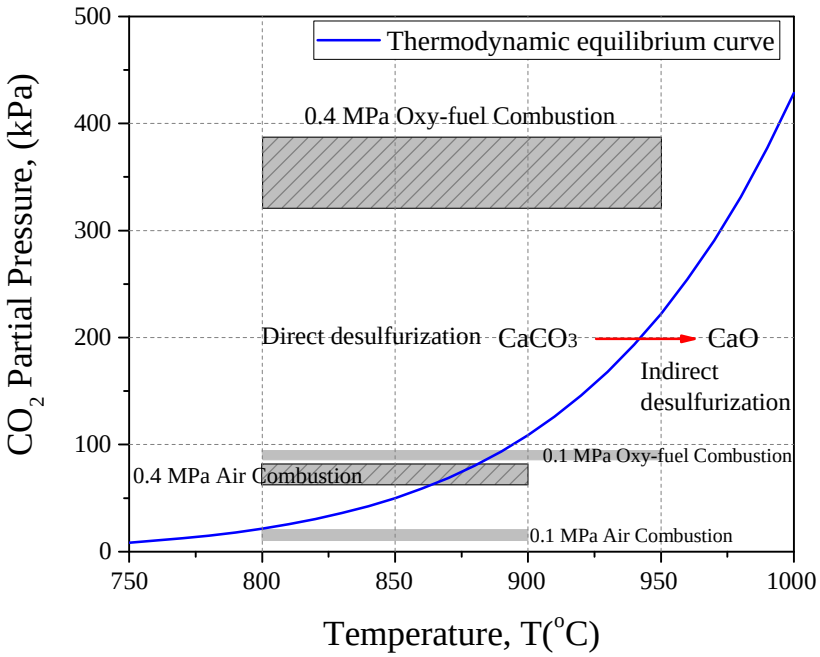

354
355 Figure 8. Thermodynamic equilibrium curve of $CaCO_3$ calcination
356
357
358

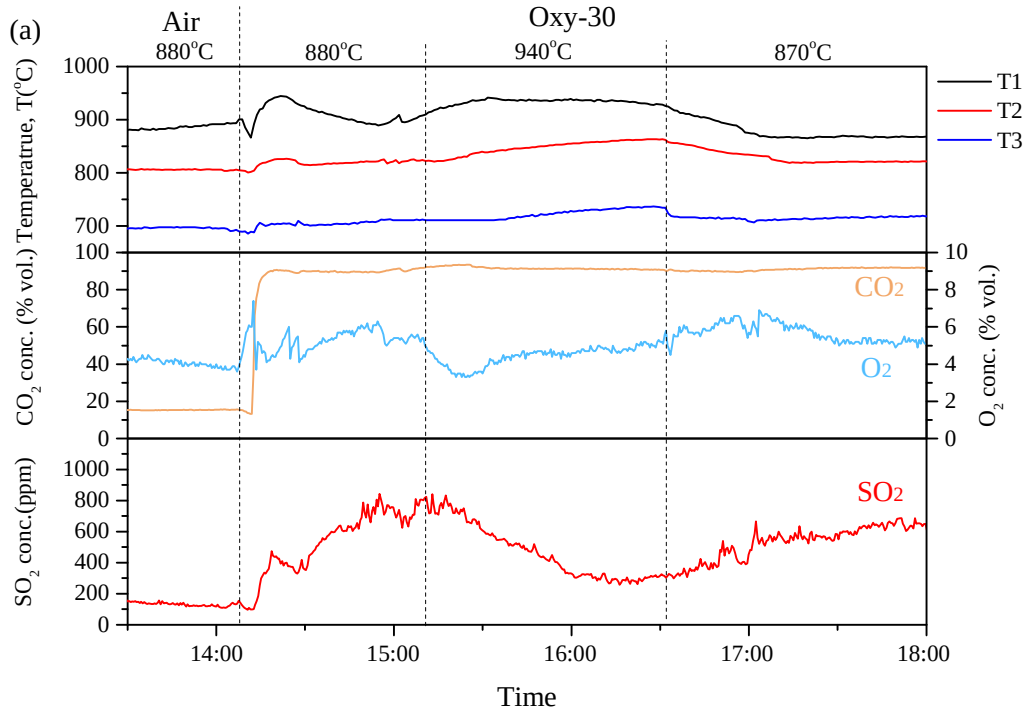

359

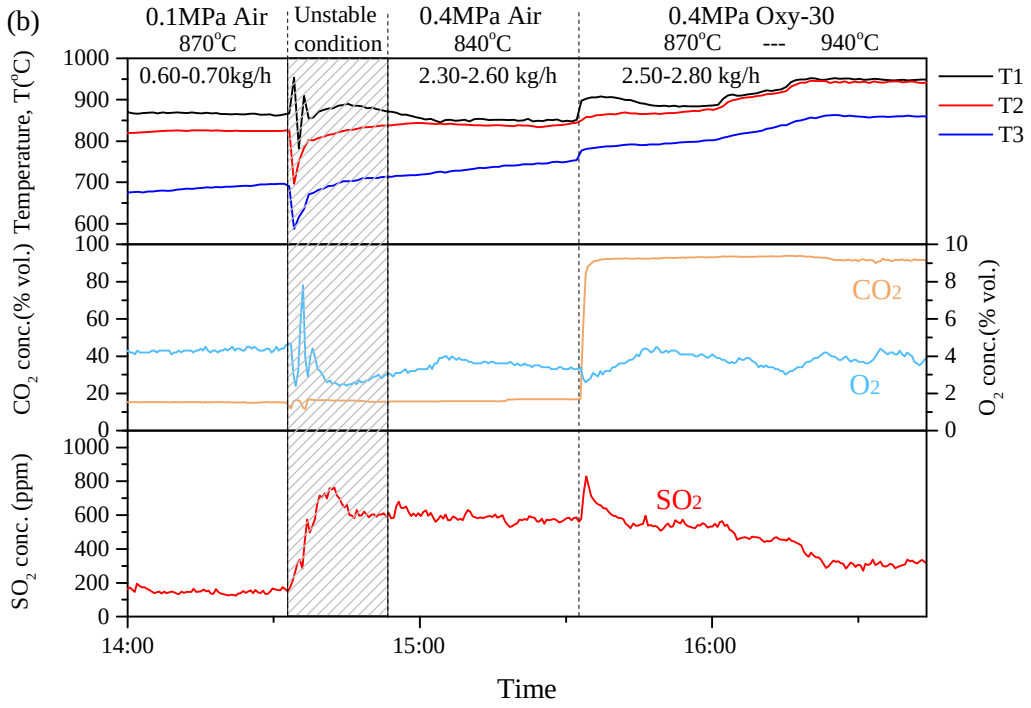

Figure 9. Real-time data of temperatures and flue gas with limestone (a) 0.1 MPa with the coal feeding rate of 0.60-0.70 kg/h (b) 0.4 MPa with the coal feeding rate of 2.50-2.80 kg/h

Fig. 9 (b) shows the desulfurization behavior of limestone under 0.4 MPa with both air and oxy-30 atmospheres. The SO_2 concentration of air combustion under 0.4 MPa (650 ppm) was higher than that under atmospheric pressure (160 ppm). Even though the CO_2 concentration was only about 15-18 vol% under the air combustion condition, the CO_2 partial pressure was increased to 60-72 kPa when the total combustion pressure quadrupled from 0.1 MPa to 0.4 MPa. Similar to oxy-fuel combustion conditions, the higher CO_2 partial pressure with the pressurized air combustion inhibited the calcination of limestone, and hence reduced the desulfurization efficiency. Fig. 10 compares the desulfurization efficiencies of limestone under different combustion pressures in both air and oxy-30 atmospheres with a bed temperature of 890 °C. The decline of the desulfurization efficiency from atmospheric air combustion to atmospheric oxy-30 combustion or pressurized air combustion was mainly caused by the transition from indirect to direct desulfurization.

In addition to the lower reaction rate of direct desulfurization, Illerup et al. [40] also found that $CaCO_3$ particles were more likely to sinter due to its lower melting temperature, which could lead to the lower degree of sulfation under uncalcined conditions. As the bed temperature of 890 ^oC was close to the critical temperature of calcination, the higher CO_2 partial pressure under the atmospheric oxy-30 combustion condition than under the pressurized air combustion condition was more adverse to the calcination, which led to a lower desulfurization efficiency with the atmospheric oxy-30 combustion. This phenomenon was also observed by Ulerich et al. [41] and Bulewicz et al. [42] who concluded that the sulfur capture capacity of limestone decreased with increasing CO_2 partial pressure under direct desulfurization conditions. The CO_2 partial pressure became much higher under the pressurized oxy-fuel combustion conditions. Specifically, with the total combustion pressure of 0.4 MPa and the CO_2 concentration of about 90 vol%, the CO_2 partial pressure reached about 340-360 kPa. Fig. 8 clearly shows that the calcination of limestone cannot occur with a reaction temperature of 940 ^oC for the oxy-fuel combustion at 0.4 MPa. In theory, the higher CO_2 partial pressure under the pressurized oxy-30 combustion condition than that under the atmospheric oxy-30 combustion condition should lead to a lower desulfurization efficiency. However, the efficiency of oxy-combustion rose from 54% to 63% after the combustion pressure was increased from 0.1 MPa to 0.4 MPa (Fig. 10). In this case, it should be noticed that the higher CO_2 partial pressure was caused by an increase in the total combustion pressure rather than the CO_2 volumetric concentration in the combustion products. Lisa and Hupa [43] investigated the effect of total pressure on the sulfation of two different limestone (with air atmosphere) by using a pressurized thermogravimetric analyzer, and found that an increase in the total pressure from 1.0 MPa to 2.5 MPa promoted the conversion of $CaCO_3$ to $CaSO_4$ through the route of

direct desulfurization. The experimental results of this study confirmed that a higher total pressure was beneficial to the direct desulfurization of oxy-fuel combustion in a fluidized bed combustor, even though the CO_2 partial pressure was increased proportionally to the total pressure. Therefore, although increases in CO_2 concentration and combustion pressure can both increase the CO_2 partial pressure, their effects on the direct desulfurization efficiency are different. With a given combustion pressure, an increase in CO_2 concentration decreases the direct desulfurization efficiency of limestone. Conversely, an increase in combustion pressure increases the direct desulfurization efficiency if the CO_2 concentration is fixed.

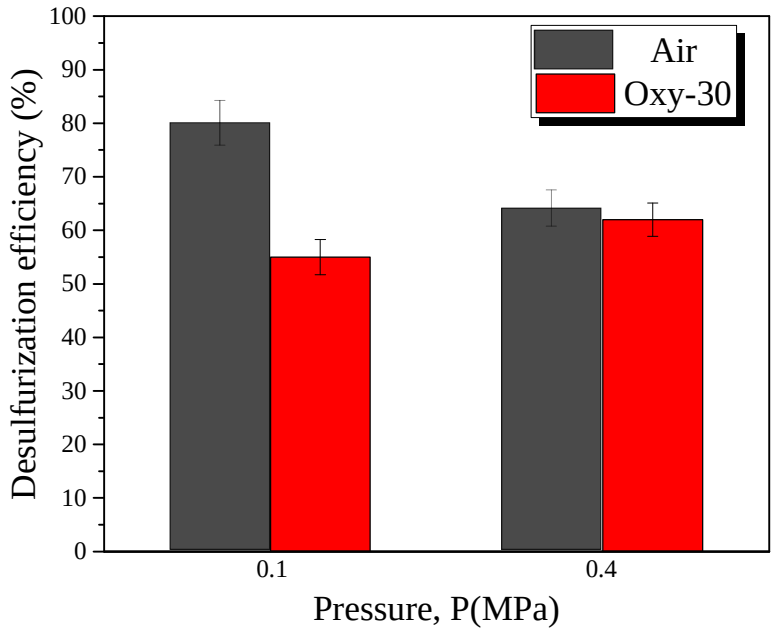

Figure 10. Desulfurization efficiency of limestone at bed temperature of 890 °C

Fig. 11 shows the effects of temperature on the desulfurization efficiency under different combustion pressures and atmospheres. Under the atmospheric air combustion conditions, the optimum temperature of indirect desulfurization was about 840 °C which agreed with previous studies [41, 43]. When the temperature was increased to

890 °C, a slight decline of efficiency was observed, and this could be due to that the higher temperature increased the number of pores in the particle surface but reduced their sizes, which made it easier for them to be blocked by the product layer of $CaSO_4$ [41, 43].

When the oxidant was switched from air to oxy-30 or the pressure was increased from 0.1 MPa to 0.4 MPa, the calcination of limestone did not occur if the temperature was below 900 °C, and the sulfation mechanism was shifted from indirect to direct desulfurization. Fig. 11 shows that all of the direct desulfurization efficiencies of different combustion conditions were lower than the indirect desulfurization efficiencies of atmospheric air combustion. With a bed temperature of 840 °C, the direct desulfurization efficiency varied between 40-50% whereas the indirect desulfurization efficiency under atmospheric air combustion condition was about 80%. Fig. 11 clearly shows that the effect of the temperature increment from 840 °C on the direct desulfurization efficiency was very different from that on the indirect desulfurization of air combustion at atmospheric pressure. All of the direct efficiencies increased by about 15%, whereas the indirect efficiency remained more or less at 80%, when the bed temperature was increased from 840 °C to 890 °C. The promoting effect of the temperature increase on the direct desulfurization efficiency was mainly attributed to the combination of the higher direct desulfurization reaction rate and the larger effective diffusivity of SO_2. The same promoting effect was observed previously with pressurized air combustion [43] and atmospheric oxy-fuel combustion [44]. The results obtained in this study confirm that higher combustion temperatures also enhance the direct desulfurization in the pressurized oxy-fuel fluidized bed combustion. Fig. 11 also shows that when the temperature was below 900 °C, the desulfurization efficiency of the pressurized oxy-30 combustion (0.4 MPa) was higher than that of the atmospheric

444 oxy-30 combustion. This agrees with the conclusion derived from the results shown in
445 Fig. 10 and by other researchers [43] that an increase in combustion pressure increases
446 the direct desulfurization efficiency. A further increase in bed temperature to 940 ^{o}C
447 allowed the limestone to calcine under the atmospheric oxy-30 combustion condition,
448 and the transition from direct to indirect desulfurization led to a higher desulfurization
449 efficiency. According to the thermodynamic equilibrium curve shown in Fig. 8, the
450 calcination of limestone cannot occur under the pressurized oxy-30 combustion
451 condition (0.4 MPa) with a bed temperature of 940 ^{o}C, and the direct desulfurization
452 efficiency should be much lower than the indirect desulfurization efficiency under the
453 conditions of 0.1 MPa and oxy-30. However, the direct desulfurization efficiency (0.4
454 MPa, oxy-30, 940 ^{o}C) reached 79% which was just 2% less than that of the indirect
455 desulfurization efficiency (0.1 MPa, oxy-30, 940 ^{o}C). In this case, the positive effect of
456 higher pressure on direct desulfurization narrowed the desulfurization efficiency gap,
457 and the desulfurization efficiency of limestone in pressurized oxy-coal combustion
458 became comparable to that in atmospheric oxy-coal combustion with a reaction
459 temperature of 940 ^{o}C.

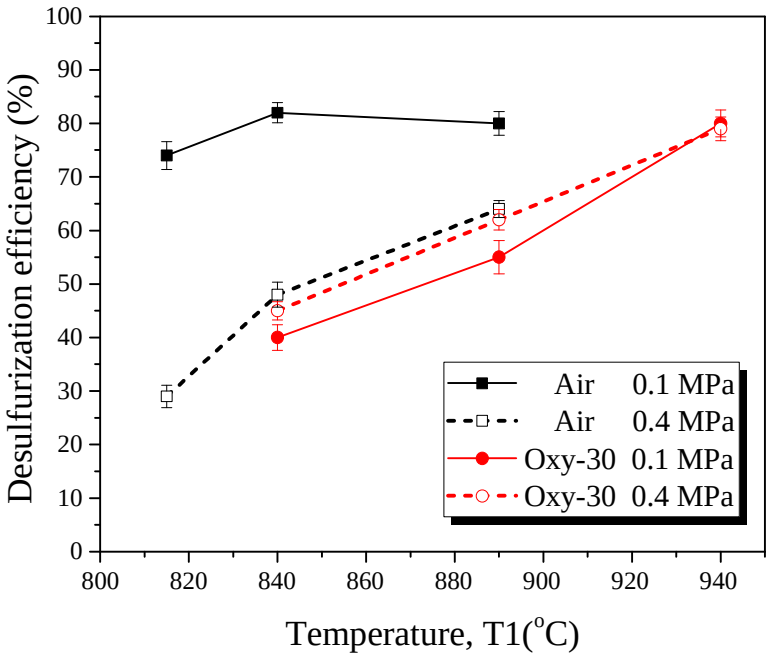

Figure 11. Effect of temperature on desulfurization efficiency

3.3 Surface structure of limestone

As many previous studies showed that the surface structure of sorbents determined the desulfurization rate and efficiency [24-25, 44], it is important to investigate the effects of combustion pressure, temperature and atmosphere on the surface structure of limestone in this study. Because the product of limestone can hardly be separated from ashes or bed materials after the fluidized bed combustion experiments, the limestone product samples were prepared in a tube furnace under similar reaction conditions to those in the fluidized bed combustor. Although the limestone particles in the tube furnace were static and there was a lack of particle to particle collisions, the results of the tube furnace experiments should still be helpful for us to understand the calcination and desulfurization behaviors of limestone in the fluidized bed combustor.

Fig. 12 shows the SEM images of particle surface under different reaction conditions without SO_2. Fig. 12 (a) presents the surface of a raw limestone particle, and it can be seen that the surface was largely non-porous. Fig. 12 (b) shows the surface of

particles under a typical air combustion condition, and many pores was seen on the surface as a result of the CO_2 release during the calcination of limestone. These pores on the surface increase the specific surface area of the particles and accelerate the desulfurization rate, which explained the higher desulfurization efficiency of air combustion (Fig. 11). Fig. 12 (c), (d) and (e) depict the surface structures of the limestone particles under the atmospheric oxy-30 combustion condition at 850, 900 and 950 ^{o}C, respectively. As shown in Fig. 8, the calcination of limestone cannot occur under the atmospheric oxy-30 combustion condition at a bed temperature of 850 ^{o}C, and no pore was observed on its surface (Fig. 12 (c)). With an increase in temperature from 850 ^{o}C to 950 ^{o}C under the atmospheric oxy-30 condition, more and more pores appeared on the surface (Fig. 12 (d) - (e)), which indicated the calcination occurred. These SEM images confirmed the analysis in section 3.2 that the higher desulfurization efficiency with an increase in temperature under the oxy-combustion condition was caused by the transition from direct desulfurization to indirect desulfurization. Fig. 12 (f), (g) and (h) show the surfaces of sorbent particles under the conditions of oxy-30 combustion at 0.4 MPa with different temperatures. According to the thermodynamic equilibrium curve shown in Fig. 8, the calcination of limestone under the condition of oxy-30 combustion at 0.4 MPa will not occur even the temperature reaches 950 ^{o}C. Compared with Figs. 12 (d) and (e), Figs. 12 (g) and (h) had fewer pores, hence indicating the higher combustion pressure indeed inhibited the calcination of limestone. Besides, these SEM images also show the sintering conditions of the limestone particle surfaces. The surface of the limestone particles under the atmospheric air combustion condition (Fig. 12 (b)) was smooth, and no edge or corner could be observed. However, the surfaces (Fig. 12 (c)) under the atmospheric oxy-30 combustion condition at the same reaction temperature (850 ^{o}C) showed no sign of sintering and looked like almost

502 the same as the surface of raw limestone particles (Fig. 12(a)). This seems to be
503 contradicting with the fact that $CaCO_3$ has a lower melting temperature (1339 ^oC) than
504 that of CaO (2572 ^oC), and further research is needed to clarify this. With an increase
505 in temperature from 850 ^oC to 950 ^oC, sintering phenomena were observed on the
506 surfaces (Figs 12. (d) - (h)) of limestone particles under the conditions of oxy-30
507 combustion at both 0.1 MPa and 0.4 MPa.

508 Fig 13 shows the specific surface area (BET surface area) of sorbent particles
509 under different reaction conditions. The raw limestone sample had a specific surface
510 area of 0.49 m^2/g but the surface area increased significantly to 15.23 m^2/g after the
511 calcination under the atmospheric air combustion condition at 850 ^oC. The specific
512 surface area of the limestone particles under the atmospheric oxy-30 combustion or the
513 pressurized (0.4 MPa) combustion condition at 850 ^oC was seen to be very similar to
514 that of the raw limestone particle (0.4 MPa), and this indicates that the calcination of
515 limestone did not occur under the condition. When the temperature was raised to 900
516 ^oC, the surface area under the condition of atmospheric oxy-30 combustion and 0.4 MPa
517 air combustion condition increased to 4.78 m^2/g and 2.45 m^2/g respectively, which
518 indicates the occurrence of calcination. With a further temperature increase to 950 ^oC,
519 the specific surface area with the atmospheric oxy-30 combustion reached about 13.9
520 m^2/g which was close to that of atmospheric air combustion at 850 ^oC. The increase of
521 specific surface area with temperature (Fig. 13) showed the same pattern as the
522 desulfurization efficiency (Fig. 11). Under the pressure of 0.4 MPa and oxy-30
523 atmosphere, the specific surface area of the limestone particles remained almost
524 constant when the temperature was increased from 850 to 950 ^oC, which agreed with
525 the results of SEM images (Figs. 12 (g – h)) and the thermodynamic equilibrium curve
526 in Fig. 8 that almost no calcination occurred.

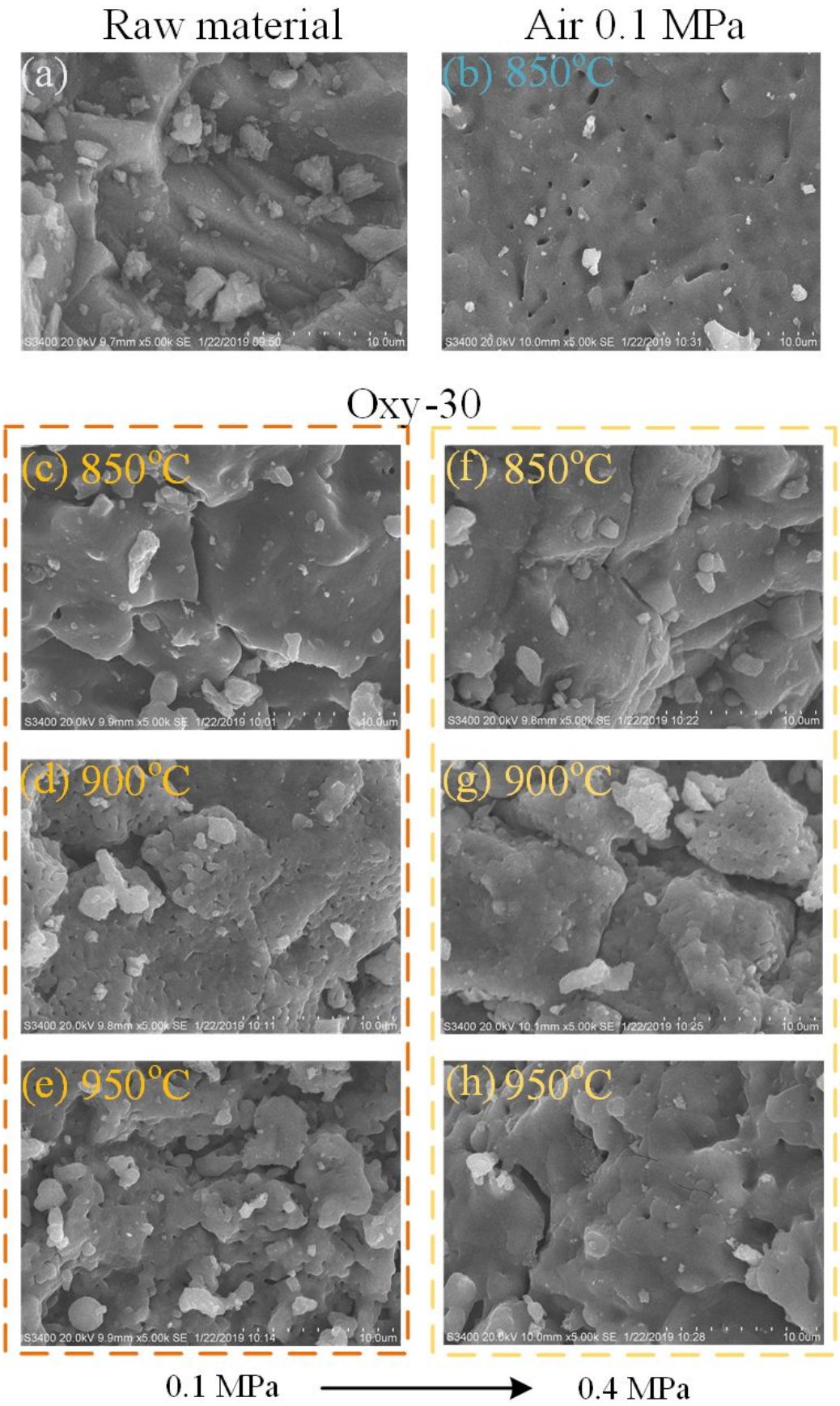

Figure 12. SEM photographs of particle surface of (a) Raw limestone (b) 0.1 MPa, air, 850°C (c) 0.1 MPa, oxy-30, 850°C (d) 0.1 MPa, oxy-30, 900°C (e) 0.1 MPa, oxy-30,

950°C (f) 0.4 MPa, oxy-30, 850°C (g) 0.4 MPa, oxy-30, 900°C (h) 0.4 MPa, oxy-30, 950°C without SO_2

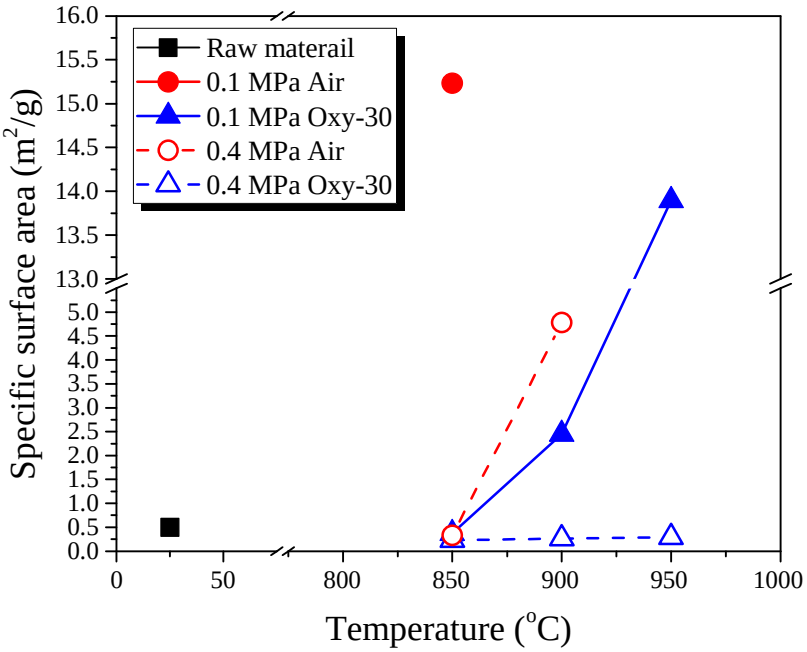

Figure 13. Specific surface area of sorbent particle

Fig. 14 shows the SEM images of the limestone product surfaces under different reaction conditions with the presence of SO_2 (1000 ppm). The main difference in the reaction conditions between the tests of Fig. 12 and Fig. 14 was the introduction of SO_2. Compared Fig. 14 with Fig. 12, it is clear that a product layer was generated on the outer surface of the particles, which was caused by the higher molar fraction of $CaSO_4$ than CaO and $CaCO_3$ [45]. As mentioned above, an increase in temperature from 850 °C to 950 °C under the atmospheric oxy-30 condition leads to the transition from direct to indirect desulfurization of limestone, and Fig. 14 (b) has fewer pores over the entire surface than Fig. 14 (a). It should be noticed that the fewer pores on the surface with indirect desulfurization doesn't mean the less formation of pores during the whole process. Conversely, more pores appeared on the surface at the early stage due to the release of CO_2 (Fig. 12 (e) has more pores than Fig. 12 (c)). However, the formation rate of $CaSO_4$ by indirect desulfurization was much faster than that of direct

desulfurization, resulting in plugging of pores and formation of a dense product layer on the surface [14] (Fig. 14 (b) has fewer pores over the entire surface than Fig. 14 (a)). Under the pressure of 0.4 MPa, the limestone was still non-calcining when the reaction temperature was increased to 950 °C, but the fewer pores on the surface in Fig. 14 (d) than Fig. 14 (c) caused by the coverage of $CaSO_4$ product layer indicated that the direct desulfurization rate increased significantly with temperature, which can also explain the high desulfurization efficiency at 950 °C (Fig. 11).

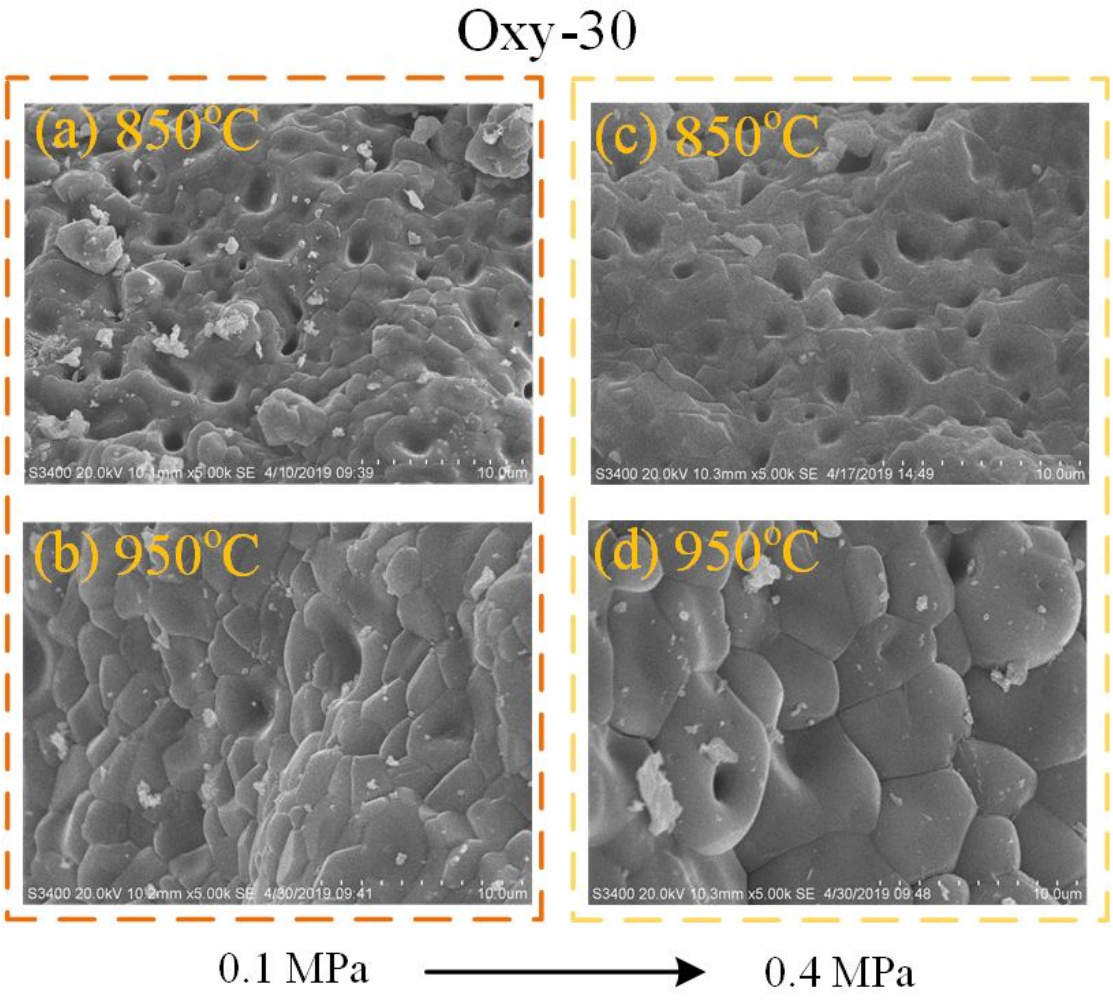

Figure 14. SEM photographs of particle surface of (a) 0.1 MPa, oxy-30, 850°C (b) 0.1 MPa, oxy-30, 950°C (c) 0.4 MPa, oxy-30, 850°C (d) 0.4 MPa, oxy-30, 950°C with SO_2

4. Conclusions

Experiments focusing on SO_2 emissions and the desulfurization of limestone were carried out in a 30 kW_{th} pressurized fluidized bed combustor under both air and oxy-fuel combustion conditions. The effects of combustion pressure, atmosphere and temperature on SO_2 emissions and desulfurization efficiency of limestone were thoroughly investigated. Scanning electron microscopy (SEM) imaging and nitrogen adsorption analysis were applied to study the surface structures of limestone products. The following conclusions can be drawn from the experimental results:

(1) SO_2 emissions were almost independent of combustion pressure and excess oxygen coefficient under both air and O_2/CO_2 combustion atmospheres.

(2) Under both atmospheric and pressurized combustion conditions, SO_2 emissions from air combustion were about 15-20 % higher than those from oxy-30 combustion atmosphere as more sulfur was retained in the fuel ashes produced by the oxy-30 combustion.

(3) Under the conditions of this study, with a given combustion pressure, an increase in CO_2 concentration decreased the direct desulfurization efficiency of limestone. Conversely, an increase in combustion pressure increased the direct desulfurization efficiency if the CO_2 concentration was fixed.

(4) An increase in bed temperature from 850 ^oC to about 950 ^oC significantly improved the desulfurization efficiency of limestone in oxy-coal combustion. With the same bed temperature of about 950 ^oC, the direct desulfurization efficiency of the pressurized oxy-coal combustion (0.4 MPa) was comparable to the indirect desulfurization efficiency of atmospheric oxy-coal combustion.

(5) The SEM images and BET surface areas of the reacted limestone particles confirmed that the calcination of limestone could not occur under the pressurized oxy-

coal combustion condition (0.4 MPa, Oxy-30) with a bed temperature of about 950 ^{o}C, and hence the desulfurization proceeded through the direct desulfurization reaction route. However, the surface morphology of the reacted limestone particles was similar to that of indirect desulfurization under the atmospheric oxy-coal combustion condition due to the high formation rate of $CaSO_4$ product layer under the pressurized oxy-coal combustion condition (0.4 MPa, Oxy-30, 950 ^{o}C).

The results of this study have shown that limestone can still be used as an effective SO_2 sorbent under the pressurized oxy-coal combustion conditions as long as the combustion temperature is raised to about 950 ^{o}C from the normal atmospheric FB combustion temperature at ca. 850 ^{o}C. Our future work will focus on the investigation of the effectiveness and mechanism of dolomite in capturing SO_2 under the pressurized oxy-coal combustion conditions at different combustion temperatures. Limestone is the most frequently used SO_2 sorbent for FB combustion because of its excellent availability and lower cost, whereas dolomite is recommended for pressurized fluidized bed combustion due to the beneficial roles of $MgCO_3$ to capture SO_2 at high pressure [45-47].

Acknowledgement

Funding: This work was supported by National Key Research and Development Program of China (2016YFB0600802), National Natural Science Foundation of China (Key Program, 51736002), Key Research and Development Program of Jiangsu Province (BE2017195) and Scientific Research Foundation of Graduate School of Southeast University (YJBB1810).

References

[1] Chen L, Yong S Z, Ghoneim A F. Oxy-fuel combustion of pulverized coal: characterization, fundamentals, stabilization and CFD modeling. Prog. Energy combust. Sci. 2012, 38 (2), 156-214.

614 [2] Mathekga H I, Oboirien B O, North B C. A review of oxy-fuel combustion in
615 fluidized bed reactors. Int. J. Energy. Res. 2016, 40, 878-902.
616 [3] Scheffknecht G, AI-Makhadmeh L, Schnell U, Maier J. Oxy-fuel coal combustion-
617 A review of the current state of the art. Int. J. Greenh. Gas Control 2011, 5, S16-35.
618 [4] Toftegaard M, Brix J, Jensen P, Glarborg P, Jensen A. Oxy-fuel combustion of solid
619 fuels. Prog. Energy Combust. Sci. 2010, 36(5), 581-625.
620 [5] Koornneef J, Junginger M, Faaij A. Development of fluidized bed combustion-an
621 overview of trends, performance and cost. Prog. Energy Combust. Sci. 2007, 33(1), 19-
622 55.
623 [6] Tranier J, Dubettier R, Darde A, Perrin N. Air separation, flue gas compression
624 and purification units for oxy-coal combustion systems. Energy Proc. 2011, 4, 966-971.
625 [7] Hong J, Field R, Gazzino M, et al. Operating pressure dependence of the
626 pressurized oxy-fuel combustion power cycle. Energy 2010, 35 (12), 5391-5399.
627 [8] Gopan A, Kumfer B M, Phillips J, Thimsen D, Smith R, Axelbaum R L. Process
628 design and performance analysis of a Staged, Pressurized Oxy-Combustion (SPOC)
629 power plant for carbon capture. Appl. Energy 2014, 125, 179-188.
630 [9] Zebian H, Gazzino M, Mitsos A. Multi-variable optimization of pressurized oxy-
631 coal combustion. Energy 2012, 38 (1), 37-57.
632 [10] Hagi H, Nemer M, Moullec Y L, et al. Towards second generation oxy-pulverized
633 coal power plants: energy penalty reduction potential of pressurized oxy-combustion
634 systems. Energy Procedia. 2014, 63, 431-439.
635 [11] Pang L, Shao Y, Zhong W, Liu H. Experimental investigation on the coal
636 combustion in a pressurized fluidized bed. Energy 2018, 165, 1119-1128.
637 [12] Saastamoinen J J, Aho M J, Hamalainen J P, Hernberg R, Joutsenoja T. Pressurized
638 pulverized fuel combustion in different concentrations of oxygen and carbon dioxide.
639 Energy Fuels 1996, 10, 121-133.
640 [13] Lasek J A, Janusz M, Zuwała J, Glod K, Iluk A. Oxy-fuel combustion of selected
641 solid fuels under atmospheric and elevated pressures. Energy 2013, 62, 105-112.
642 [14] Gomez M, Fernandez A, Llavona I, Kuivalainen R. Reprint of “experiences in
643 sulphur capture in a 30 MWth circulating fluidized bed boiler under oxy-combustion
644 conditions”. Appl. Therm. Eng. 2015, 74, 69-74.
645 [15] Duan L, Sun H, Zhao C, Zhou W, Chen X. Coal combustion characteristics on an
646 oxy-fuel circulating fluidized bed combustor with warm flue gas recycle. Fuel 2014,
647 127, 47-51.

[16].Tan Y, Croiset E, Douglas M A, Thambimuthu K V. Combustion characteristics of coal in a mixture of oxygen and recycled flue gas. Fuel 2006, 85, 507-512.

[17] Zou C, Huang Z, Xiong J. A pilot scale study on co-capture of SO_2 and NO_X in O_2/CO_2 recycled coal combustion and techno-economic evaluation. Science China Technological Sciences 2010, 53(1), 155-159.

[18] Croiset E, Thambimuthu K V. NOx and SO_2 emissions from O_2/CO_2 recycle coal combustion. Fuel 2001, 80, 2117-2121.

[19] Fleig D, Andersson K, Johnsson F, Leckner B. Conversion of sulfur during pulverized oxy-coal combustion. Energy Fuels 2011, 25, 647-655.

[20] Liu H, Zailani R, Gibbs B M. Comparisons of pulverized coal combustion in air and in mixtures of O_2/CO_2. Fuel 2005, 84, 833-840.

[21] Tan L, Li S, Li W, Effects of oxygen staging and excess oxygen on O_2/CO_2 Combustion with a high oxygen concentration in a circulating fluidized bed. Energy Fuels 2014, 28, 2069-2075.

[22] Czakiert T, Muskala W, Jankowska S, Krawcsyk G, Borecki P, Jesionowski L, Nowak W. Combustible matter conversion in an oxy-fuel circulating fluidized-bed (CFB) environment. Energy Fuels 2012, 26, 5437-5445.

[23] Hu Y, Naito S, Kobayashi N, Hasatani M. CO_2, NO_x and SO_2 emissions from the combustion of coal with high oxygen concentration gases. Fuel 2000, 79, 1925-1932.

[24] Jeong S, Lee K, Keel S, Yun J, Kim Y, Kim S. Mechanisms of direct and in-direct sulfation of limestone. Fuel 2015, 161, 1-11.

[25] Kim Y B, Gwak Y R, Keel S I, Yun J H, Lee S H. Direct desulfurization of limestones under oxy-circulating fluidized bed combustion conditions. Chem. Eng. J. XXX, XXXX, XXX-XXX

[26] de Diego L, de Obras-loscertales M, Rufas A, Garacia-Labiano F, Gayan P, Abad A, Adanez J. Pollutant emissions in a bubbling fluidized bed combustor working in oxy-fuel operating conditions: effect of flue gas recirculation. Appl. Energy, 2013, 102, 860-867.

[27] Lupianez C, Guedea I, Bolea I, Diez L I, Romeo L M. Experimental study of SO_2 and NOx emissions in fluidized bed oxy-fuel combustion. Fuel Process. Technol. 2013, 106, 587-594.

[28] Jia L, Tan Y, Anthony E J. Emissions of SO_2 and NO_x during oxy-fuel CFB combustion tests in a mini-circulating fluidized bed combustion reactor. Energy Fuels 2010, 24, 910-915.

682 [29] Tan Y, Jia L, Wu Y, Anthony E J. Experiences and results on a 0.8 MW_{th} oxy-fuel
683 operation pilot-scale circulating fluidized bed, Appl. Energy 2012, 92, 343-347.
684 [30] Zevenhoven R, Yrjas P, Hupa M. Sulfur dioxide capture under PFBC conditions:
685 the influence of sorbent particle structure. Fuel 1998, 77(4), 285-292.
686 [31] Garcia-Labiano F, Rufas A, de Diego L F, de las Obras-Loscertales M, Gayan P,
687 Abad A, Adanez J. Calcium-based sorbents behavior during sulphation at oxy-fuel
688 fluidized bed combustion conditions. Fuel 2011, 90, 3100-3108.
689 [32] de Diego L F, Obras-Loscertales M d, Garcia-Labiano F, Rufas A, Abad A, Gayan
690 P, Adanez J. Characterization of a limestone in a batch fluidized bed reactor for sulfur
691 retention under oxy-fuel operating conditions. Int. J. Greenh. Gas Control 2011, 5,
692 1190-1198
693 [33] Pang L, Shao Y, Zhong W, Liu H, Jiang P. An experimental investigation of oxy-
694 coal combustion in a 15 kW_{th} pressurized fluidized bed combustor. Energy Fuels 2019,
695 33, 1694-1703.
696 [34] Zhou G, Zhong W, Yu A, Dou Y, Yin J. Experimental study on characteristics of
697 pressurized grade conversion of coal. Fuel 234, 965-973.
698 [35] Czakiert T, Sztekler K, Karski S, Markiewicz D, Nowak W. Oxy-fuel circulating
699 fluidized bed combustion in a small pilot-scale test rig. Fuel Process. Technol. 2010, 91,
700 1617-1623.
701 [36] Rohan S, Terry W. Sulphur impacts during pulverized coal combustion in oxy-fuel
702 technology for carbon capture and storage. Prog. Energy Combust. 2011, 37, 69-88
703 [37] Duan Y, Duan L,Wang J, Anthony E. Observation of simultaneously low CO, NO_x
704 and SO_2 emission during oxy-coal combustion in a pressurized fluidized bed. Fuel 2019,
705 242(15), 374-381.
706 [38] Wang X, Adeosun A, Yablonsky G, Gopan A, Du P, Axelbaum RL. Synergistic
707 SO_x/NO_x chemistry leading to enhanced SO_3 and NO_2 formation during pressurized
708 oxy-combustion. React Kinet. Mech. Catal. 2018, 123, 313–22.
709 [39] Lupianez C, Diez L I, Romeo L M. NO emissions from anthracite oxy-firing in a
710 fluidized-bed combustor: effect of the temperature, limestone and O_2. Energy Fuels.
711 2013, 27, 7619-7627.
712 [40] Illerup J, Dam-Johansen K, Lunden K. High-temperature reaction between sulfur
713 dioxide and limestone-VI. The influence of high pressure. Chem. Eng Sci 1993, 48(11),
714 2151-2157.
715 [41] Ulerich N, Newby R, Keairns D. A thermogravimetric study of the sulfation of

716 limestone and dolomite-production of pressurized and atmospheric fluidized bed
717 desulfurization. Thermochimica. Acta 1980, 36, 1-6.
718 [42] Bulewics E, Kandefer S, Jurys C. Desulfurization during the fluidized combustion
719 of coal using calcium-based sorbents at pressures up to 600 kPa. J. Inst. Energy, 59,
720 188-195.
721 [43] Iisa K, Hupa M. Sulphur absorption by limestone at pressurized fluidized bed
722 conditions. Symposium on Combustion, 1991, 23(1), 943-948.
723 [44] Li W, Li S, Xu M, Wang X. Study on the limestone sulfation behavior under oxy-
724 fuel circulating fluidized bed combustion condition. J. Energy Inst. 2018, 91, 358-368.
725 [45] de las Obras-Loscertales M, Rufas A, de Diego L, Garcia-Labiano F, Gayan P,
726 Abad A, Adanez J. Morphological analysis of sulfated Ca-based sorbents under
727 conditions corresponding to oxy-fuel fluidized bed combustion, Fuel 2015, 162, 264–
728 327.
729 [46] Isabel Guedea, Irene Bolea, Carlos Lupiañez, Luis M. Romeo and Luis I. Diez.
730 Recent Technologies in Capture of CO_2. 1st ed. Sharjah: Bentham Science Publishers
731 Ltd. 2014.
732 [47] de las Obras-Loscertales M, de Diego L, Garcia-Labiano F, Rufas A, Gayan P,
733 Adanez J. Sulfur retention in an oxy-fuel bubbling fluidized bed combustor: Effect of
734 coal rank, type of sorbent and O2/CO2 ratio, Fuel 2014, 137, 384-392.